THE ASTROPHYSICAL JOURNAL, 563:L000–L000, 2001 December 10

A CORRELATION BETWEEN GALAXY LIGHT CONCENTRATION AND SUPERMASSIVE BLACK HOLE MASS

ALISTER W. GRAHAM,[1] PETER ERWIN,[2] N. CAON, AND I. TRUJILLO
Instituto de Astrofísica de Canarias, La Laguna, E-38200 Tenerife, Spain; agraham@ll.iac.es, erwin@ll.iac.es, ncaon@ll.iac.es, itc@ll.iac.es

Received 2001 September 14; accepted 2001 November 6

ABSTRACT

We present evidence for a strong correlation between the concentration of bulges and the mass of their central supermassive black hole (M_{bh})—more concentrated bulges have more massive black holes. Using $C_{r_e}(1/3)$ from Trujillo, Graham, & Caon as a measure of bulge concentration, we find that $\log (M_{bh}/M_{\odot}) = 6.81 (\pm 0.95) C_{r_e}(1/3) + 5.03 \pm 0.41$. This correlation is shown to be marginally stronger (Spearman's $r_s = 0.91$) than the relationship between the logarithm of the stellar velocity dispersion and $\log M_{bh}$ (Spearman's $r_s = 0.86$) and has comparable or less scatter (0.31 dex in $\log M_{bh}$, which decreases to 0.19 dex when we use only those galaxies whose supermassive black hole radii of influence are resolved and we remove one well-understood outlying data point).

Subject headings: black hole physics — galaxies: fundamental parameters — galaxies: kinematics and dynamics — galaxies: nuclei — galaxies: photometry — galaxies: structure

1. INTRODUCTION

Observations over the last few years have established that supermassive black holes (SMBHs; $\sim 10^6$–$10^9\ M_{\odot}$) are a common, if not universal, feature at the center of elliptical galaxies and the bulges of early-type spirals (Kormendy & Richstone 1995; Magorrian et al. 1998). Initial correlations between the masses of SMBHs and the absolute *B*-band luminosities of the host bulges[3] had a large scatter (~0.5–0.6 dex in $\log M_{bh}$, but see McLure & Dunlop 2001), which could not be accounted for by the assumed measurement errors. Subsequent studies uncovered a stronger correlation between the mass of the SMBH and the stellar velocity dispersion of the bulge, with considerably smaller scatter: only ~0.3 dex in $\log M_{bh}$ (Ferrarese & Merritt 2000; Gebhardt et al. 2000). Merritt & Ferrarese (2001a) argued that the observed scatter, for a select sample of 12 galaxies thought to have the most reliable SMBH mass estimates, was fully consistent with the measurement errors alone: that is, there may be no intrinsic scatter in the correlation. This clearly suggests that a strong cross talk exists—or once existed—between the central black hole and its host bulge. The reasons for this and the presumed formation mechanism are, however, not well understood, although many possibilities have been put forward (see, e.g., the discussion in Merritt & Ferrarese 2001b).

Recently, Graham, Trujillo, & Caon (2001) have shown that the central concentration of bulge light, measured within 1 effective half-light radius, positively correlates with the stellar velocity dispersion of the bulge. Following up on this, we present here, for the first time, a correlation between SMBH mass and bulge concentration, showing that more concentrated bulges have more massive SMBHs. This correlation is found to be at least as strong as that between SMBH mass and stellar velocity dispersion and may have less scatter. We suggest that the bulge concentration is certainly as significant a parameter as, and one perhaps more revealing than, velocity dispersion (which presumably is a response to the underlying bulge mass distribution), for understanding the fueling and growth of central SMBHs.

2. GALAXY DATA AND MEASUREMENTS

We began with the updated list of SMBH detections and mass estimates in the first two sections of Merritt & Ferrarese's (2001b) Table 1. These black hole masses include a number of revised estimates from the "Nuker group" and Space Telescope Imaging Spectrograph (STIS) Investigation Definition Team presented by Kormendy & Gebhardt (2001). This is an initial total of 30 galaxies, including the Milky Way. The only quantity that we have changed is the SMBH mass estimate for NGC 4374. Although this object appears in the list of galaxies with "reliable" SMBH mass estimates (because the black hole's sphere of influence has been resolved), Maciejewski & Binney (2001) recently revised its mass estimate lower by a factor of 4 after taking proper account of finite slit-width effects.

We searched the various public archives for high-quality *R*-band images[4] that were large enough to guarantee good sky subtraction and that had no central saturation. We found useful images for a total of 21 galaxies, primarily from the Isaac Newton Group and *Hubble Space Telescope* (*HST*) archives, as well as images from Frei et al. (1996) and Hintzen et al. (1993), available via the NASA Extragalactic Database (NED). We were also able to use an unpublished image obtained with the WIYN Telescope for NGC 3245, and the minor-axis near-infrared surface brightness profile of the Milky Way published by Kent, Dame, & Fazio (1991), making a total of 23 galaxies with usable data.

A full discussion of the images for individual galaxies, along with reduction procedures and the extracted light profiles, analyses, and model fitting for each galaxy will be presented in P. Erwin, A. W. Graham, N. Caon, & I. Trujillo (2001, in preparation). Briefly, we fitted ellipses to the isophotes, allowing the position angle and ellipticity to vary with radius. The resulting light profiles were then fitted with a seeing-convolved[5]

[1] Department of Astronomy, University of Florida, Gainesville, FL.
[2] Guest Investigator of the UK Astronomy Data Centre.
[3] By the term "bulge," we mean both elliptical galaxies and the bulges of spiral galaxies.
[4] For three galaxies, we used *HST* F814W images instead.
[5] We used a Moffat function to describe the point-spread function; seeing full width, half-maxima were measured from stars in the individual images.

Sérsic (1968) $r^{1/n}$ model. We modeled disk galaxy profiles with a combined (seeing-convolved) exponential disk and $r^{1/n}$ bulge.

For two galaxies with strong bars, we used the light profile derived from cuts along an axis perpendicular to the bar; this produced much better fits and avoided most of the bar contribution. The inner arcsecond of the profiles was generally excluded from the fit since these regions are often dominated by relatively flat cores, bright nuclear disks, or nuclear point sources (e.g., Rest et al. 2001, and references therein), none of which can be modeled with Sérsic profiles. We are thus measuring the overall concentration of the bulge, independent of any separate central stellar components such as nuclear disks. Only two galaxies could not be successfully modeled. The final set of 21 galaxies with well-fitted profiles is given in Table 1.

We then computed the concentration of the best-fitting $r^{1/n}$ models using the central concentration index first presented in Trujillo, Graham, & Caon (2001) and further developed in Graham et al. (2001). This index measures the light concentration within a bulge's half-light radius (r_e): it is the ratio of flux inside some fraction α of the half-light radius to the total flux inside the half-light radius. For an $r^{1/n}$ model, this index can be analytically defined as

$$C_{r_e}(\alpha) = \frac{\gamma(2n,\ b_n\alpha^{1/n})}{\gamma(2n,\ b_n)}, \qquad (1)$$

where n is the shape parameter of the $r^{1/n}$ model and b_n is derived numerically from the expression $\Gamma(2n) = 2\gamma(2n,\ b_n)$ in which $\Gamma(a)$ and $\gamma(a,\ x)$ are, respectively, the gamma function and the incomplete gamma function (Abramowitz & Stegun 1964).

The parameter α can be any value between 0 and 1 and defines what level of concentration is being measured. Following Graham et al. (2001), we used a value of $\alpha = 1/3$. We did, however, explore a range of values, finding that $\alpha = 1/3$ roughly produced the minimum vertical scatter in the log $M_{\rm bh}$-$C_{r_e}(\alpha)$ correlation. The quantity $C_{r_e}(1/3)$ is then simply the ratio of flux inside one-third of the half-light radius to the flux inside the entire half-light radius.

The $C_{r_e}(1/3)$ values are listed in the final column of Table 1. Because these values are analytically derived from the best-fitting Sérsic index n, the uncertainty in $C_{r_e}(1/3)$ depends directly on the uncertainty in n and is derived by standard propagation of errors. Error estimates for n are based on the results of Caon, Capaccioli, & D'Onofrio (1993), who found a typical uncertainty of ~25% when fitting with Sérsic profiles. For Sérsic values of n between 2 and 11, this corresponds to a 10%–15% uncertainty in the bulge concentration.

For comparison with the known SMBH mass–velocity dispersion relation, we also list the velocity dispersions σ_c and corresponding errors for each galaxy; these are taken from Merritt & Ferrarese (2001b) and thus incorporate the equivalent aperture correction described in Ferrarese & Merritt (2000). As Merritt & Ferrarese (2001a) showed, these values differ, on average, by only ~1% from the σ_e values used by Gebhardt et al. (2000).

TABLE 1

GALAXY PARAMETERS

Galaxy	Revised Hubble Type	σ_c (km s^{-1})	$M_{\rm bh}$ ($10^8\ M_\odot$)	n	$C_{r_e}(1/3)$
Ellipticals					
NGC 821	E6	196 ± 26	0.51 ± 0.2	4.00	$0.47^{+0.04}_{-0.06}$
NGC 3377	E5–6	131 ± 17	$1.03^{+1.6}_{-0.41}$	3.50	$0.44^{+0.04}_{-0.06}$
NGC 3379	E1	201 ± 26	1.35 ± 0.73	4.64	$0.49^{+0.05}_{-0.05}$
NGC 4261	E2–3	290 ± 38	$5.4^{+1.2}_{-1.2}$	6.16	$0.55^{+0.04}_{-0.06}$
NGC 4291	E	269 ± 35	$1.54^{+3.1}_{-0.68}$	4.48	$0.49^{+0.04}_{-0.06}$
NGC 4374	E1	286 ± 37	$4.3^{+3.2}_{-1.7}$	4.97	$0.51^{+0.04}_{-0.06}$
NGC 4473	E5	188 ± 25	$1.026^{+0.82}_{-0.71}$	3.27	$0.43^{+0.04}_{-0.06}$
NGC 4564	E6	153 ± 20	$0.57^{+0.13}_{-0.17}$	2.06	$0.34^{+0.04}_{-0.06}$
NGC 5845	E*	275 ± 36	$3.52^{+2.0}_{-0.72}$	3.22	$0.42^{+0.05}_{-0.05}$
NGC 6251	E	297 ± 39	5.9 ± 2.0	11.0	$0.65^{+0.03}_{-0.05}$
NGC 7052	E	261 ± 34	$3.7^{+2.6}_{-1.5}$	4.56	$0.49^{+0.04}_{-0.06}$
Bulges of Disk Galaxies					
NGC 1023	SB(rs)0$^-$	201 ± 14	$0.39^{+0.09}_{-0.11}$	2.37	$0.36^{+0.05}_{-0.05}$
NGC 2778[a]	E	171 ± 22	$0.20^{+0.16}_{-0.13}$	1.60	$0.29^{+0.04}_{-0.05}$
NGC 2787[b]	SB(r)0$^+$	210 ± 23	$0.41^{+0.04}_{-0.05}$	1.96	$0.33^{+0.04}_{-0.05}$
NGC 3031	SA(s)ab	174 ± 17	$0.68^{+0.07}_{-0.13}$	3.23	$0.42^{+0.05}_{-0.05}$
NGC 3245	SA(r)0	211 ± 19	2.1 ± 0.5	4.04	$0.47^{+0.04}_{-0.06}$
NGC 3384[b]	SB(s)0$^-$	151 ± 20	$0.185^{+0.072}_{-0.091}$	1.89	$0.32^{+0.04}_{-0.05}$
NGC 4258[c]	SAB(s)bc	138 ± 18	0.390 ± 0.034	2.02	$0.33^{+0.04}_{-0.05}$
NGC 4342[b]	S0$^-$	261 ± 34	$3.3^{+1.9}_{-1.1}$	5.12	$0.51^{+0.04}_{-0.05}$
NGC 7457	SA(rs)0$^-$	73 ± 10	$0.035^{+0.027}_{-0.017}$	1.81	$0.31^{+0.04}_{-0.05}$
Milky Way[d]	Sb	100 ± 20	0.0295 ± 0.0035	1.00	$0.22^{+0.03}_{-0.04}$

NOTE.—Galaxy types are from NED. Velocity dispersions and black hole masses from compilation in Merritt & Ferrarese 2001b, except SMBH mass for NGC 4374 (revised by Maciejewski & Binney 2001; updated errors from Kormendy & Gebhardt 2001). The central concentration $C_{r_e}(1/3)$ of each bulge was measured from *R*-band images, except where otherwise noted, with a 25% uncertainty assumed for n.

[a] NGC 2778 is classified as an elliptical galaxy in the NASA Extragalactic Database (NED), but its light profile clearly indicates an S0 galaxy, with both an exponential disk and a central bulge; this interpretation is supported by the kinematical study of Rix, Carollo, & Freeman 1999.

[b] *HST* F814W image.

[c] Thuan-Gunn *r* image.

[d] 2.4 μm minor-axis profile from Kent, Dame, & Fazio 1991.

3. RESULTS

Correlations between SMBH mass and bulge concentration are presented in Figure 1; for comparison, we also show the correlations between SMBH mass and velocity dispersion for the same galaxies. We used the bisector linear regression routine from Akritas & Bershady (1996) to fit a line to these correlations. Using the *orthogonal* regression analysis of Akritas & Bershady (1996) and the orthogonal distance regression routine FITEXY of Press et al. (1989)—alternative methods for data sets with errors in both variables—gave consistent results.

We computed the Pearson correlation coefficient r and Spearman rank-order correlation coefficient r_s, both of which are given in Figure 1. The Spearman coefficient is preferred as it is more robust to outliers and does not presuppose a linear relation. The best linear fit to the whole sample is $\log M_{\rm bh} = 6.81(\pm 0.95)C_{r_e}(1/3) + 5.03 \pm 0.41$.

Figure 1 shows that the correlation between black hole mass and bulge concentration is extremely good—as good as or better than that between black hole mass and velocity dispersion. In addition, the low χ^2 value of 0.82 suggests a scatter consistent with the measurement errors alone, implying negligible intrinsic scatter (as Ferrarese & Merritt 2000 claimed for the SMBH–velocity dispersion relation). This conclusion does, however, depend on how well-determined the errors are. (See P. Erwin et al. 2001, in preparation.)

Data points at the extreme ends of a correlation can be very useful for determining the true slope because of the weight they lend, but by the same token they can heavily bias the data

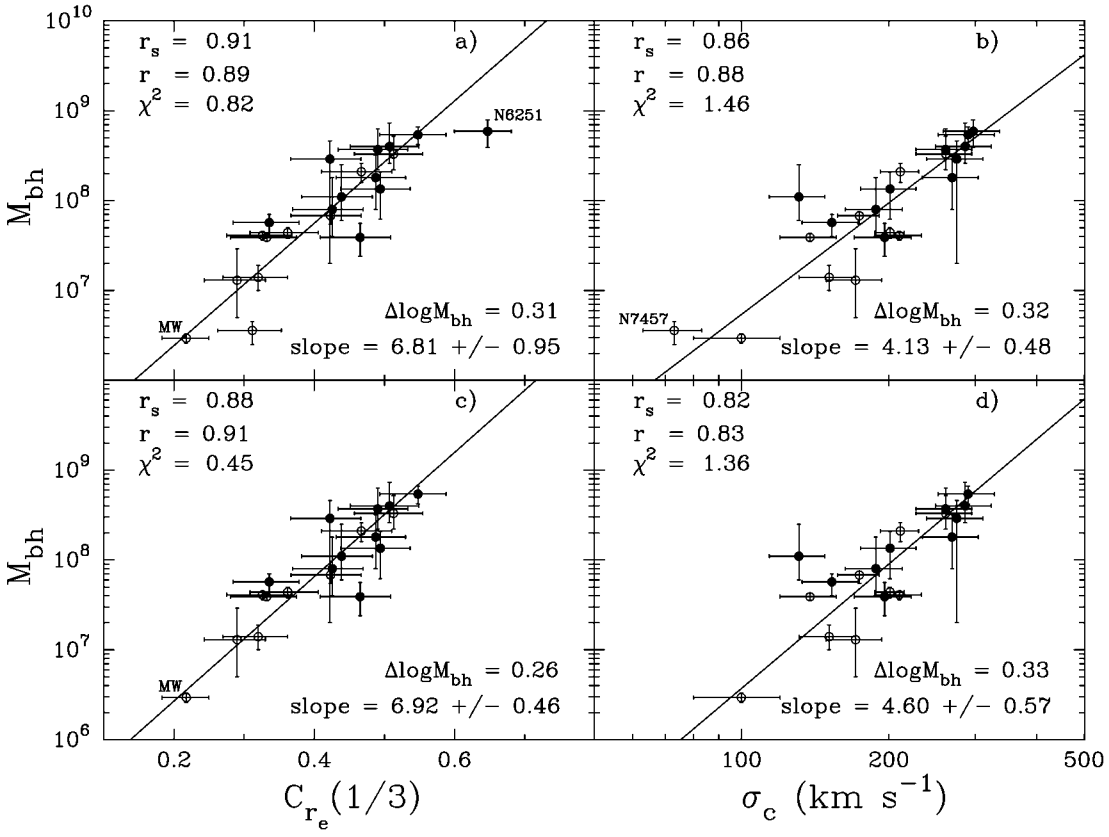

FIG. 1.—Correlations between supermassive black hole mass and (*a*) bulge concentration and (*b*) stellar velocity dispersion within $r_e/8$. Panels *c* and *d* show the correlation after removing the two outlying galaxies (NGC 7457 and NGC 6251; see § 3 and § 4). The Milky Way (MW) has been indicated. Spearman rank-order correlation coefficient r_s is given, as is the Pearson linear correlation coefficient r. The χ^2 merit function for a linear fit and the absolute vertical scatter $\Delta \log M_{\rm bh}$ are also given. Elliptical galaxies are denoted by filled circles, lenticulars and spirals by open circles.

to produce a misleading slope if they themselves have not been well measured.[6] We have identified two such potential outliers (NGC 7457 and NGC 6251) in Figure 1*a* (see § 4). We have repeated our analysis without them (Figs. 1*c* and 1*d*). In so doing, the $\log M_{\rm bh}$–$\log \sigma_c$ relation is even weaker than the $\log M_{\rm bh}$–$C_{r_e}(1/3)$ relation; it also has 27% more scatter in $\log M_{\rm bh}$.

The list of galaxies in Merritt & Ferrarese (2001b), from which we constructed our sample, was subdivided according to whether or not the black hole's sphere of influence had been resolved. Of the 22 "resolved" galaxies, we have images and useful fits for 14. We rederived the relations seen in Figure 1 using this smaller sample and found that the strength of both correlations improved; for this subsample, both correlations appear equally strong (Fig. 2).

Graham (1998) wrote, "one might expect [Sérsic's] n to correlate with the size of the black hole predicted to be at the center of many elliptical galaxies." Since $C_{r_e}(1/3)$, as defined in equation (1), is a monotonic function of the global shape parameter n (Trujillo et al. 2001), the SMBH mass–$C_{r_e}(1/3)$ correlation implies a correlation between SMBH mass and n as well. For the full galaxy sample, performing the bisector regression analysis on $\log M_{\rm bh}$ and $\log n$ (assuming a 25% error in n) gives $\log M_{\rm bh} = 2.93(\pm 0.43) \log n + 6.42 \pm 0.22$ with a scatter of 0.32 dex in $\log M_{\rm bh}$. Excluding NGC 7457 and NGC 6251 gives $\log M_{\rm bh} = 3.00(\pm 0.17) \log n + 6.45 \pm 0.11$ with a scatter of only 0.25 dex. The strength of these correlations is equal to those shown in Figures 1*a* and 1*c*.

[6] This issue is discussed at length in Merritt & Ferrarese (2001a) for one galaxy in particular—namely, the Milky Way.

4. DISCUSSION

The most significant outlier in our relation is probably NGC 6251. There is reason to believe that its concentration index may be significantly in error. The best-fitting Sérsic $r^{1/n}$ model to this galaxy has $n = 11$, which means the outer profile of this model declines slowly with radius; the observed light-profile extends to only 1 model half-light radius. The larger the value of n, the closer the $r^{1/n}$ model approaches a power law in behavior—having infinite brightness and an infinite half-light radius (e.g., Graham et al. 1996), resulting in excessively high values of $C_{r_e}(1/3)$. Values of n greater than about 10 should thus be treated with caution.

The outlying point (NGC 7457) in the lower left of Figure 1*a* is less easily dismissed and may be a true outlier worthy of individual investigation. There is some evidence for a weak bar or lens in this galaxy (Michard & Marchal 1994). While we derived a light profile perpendicular to the major axis of this feature, it does still have a finite width, which can bias our Sérsic fit to the bulge, giving a spuriously large value for n and, hence, an overestimation of the bulge concentration.

Although we cannot say which parameter [$C_{r_e}(1/3)$ or $\log \sigma$] is better, we can identify some of the advantages and disadvantages of each. Use of the concentration index for studies such as this may not be applicable to morphologically disturbed galaxies that may have undergone recent mergers or

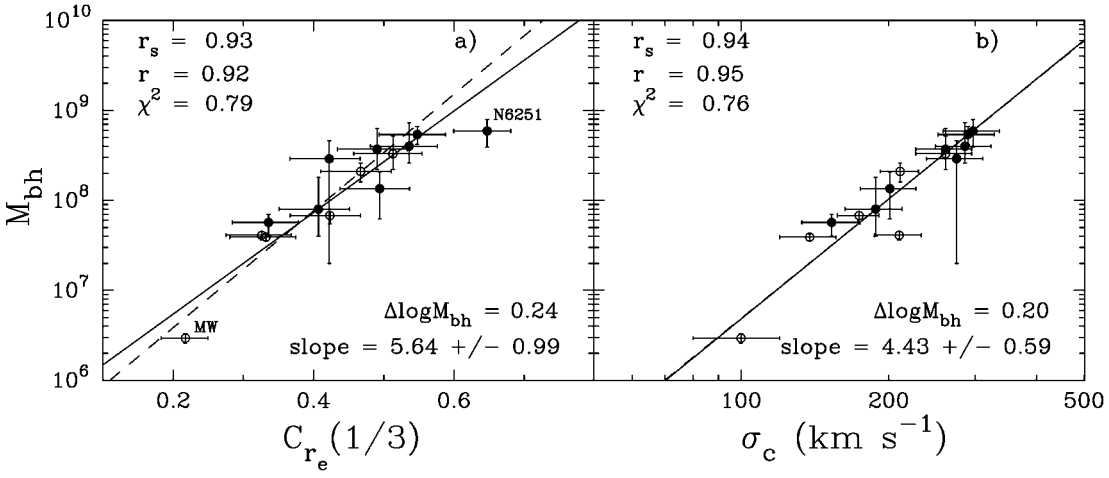

FIG. 2.—Same as Fig. 1, except using only those galaxies with resolved SMBH spheres of influence (top section of Table 1, Merritt & Ferrarese 2001b). Dashed line shows the correlation after removing NGC 6251, as done in Fig. 1. Slope to the dashed line in (*a*) is 6.49 ± 0.78 and has a vertical scatter of 0.19 dex. Slope to the dashed line in (*b*) is 4.41 ± 0.66 with a vertical scatter of 0.20 dex.

interactions (a factor that could also influence the stellar velocity dispersion). Dominant cD galaxies that have acquired large extended envelopes can also be difficult to model, and depending on the extent of the accreted material, their concentration index may be heavily biased. The stellar velocity dispersion may, on the other hand, be a more stable quantity in such cases. Velocity dispersions have additionally been measured for numerous (mostly nearby) galaxies.

One obvious, practical advantage that the concentration index has over stellar velocity dispersions is that images are far less expensive to acquire (in terms of telescope time) than stellar velocity dispersions, especially those at 1 effective radius. This is particularly important for studies of high-redshift galaxies. Second, use of the bulge concentration circumvents concerns that the SMBH may be influencing the luminosity-weighted nuclear velocity dispersion measurements (e.g., Wandel 2002). Similarly, while n and C_{r_e} are global parameters, velocity dispersion measurements are affected by kinematical substructure at the centers of bulges, rotational velocity, seeing conditions, and aperture size. It should also be noted, however, that the presence of bars, rings, and lenses within spiral galaxies can complicate the determination of the bulge concentration. A fourth advantage of the concentration index is that it can be measured from photometrically uncalibrated images; it does not rely on distance measurements, redshift-dependent corrections, or assumed mass-to-light ratios.

The bulges studied here clearly have different luminosity distributions, and unless M/L varies with radius in a very contrived fashion, they also have different mass distributions. We will never have an accurate picture of bulge formation if we continue to pigeonhole bulges into two simple classes; namely, $r^{1/4}$ and exponential.

We wish to thank Matthew Bershady for making available the linear regression code from Akritas & Bershady (1996). Based on archival data obtained with the NASA/ESA *Hubble Space Telescope* and the Isaac Newton Group of Telescopes at the Spanish Observatorio del Roque de Los Muchachos of the Instituto de Astrofísica de Canarias. This research has made use of the NASA/IPAC Extragalactic Database (NED). The WIYN Observatory is a joint facility of the University of Wisconsin–Madison, Indiana University, Yale University, and the National Optical Astronomy Observatories.

REFERENCES

Abramowitz, M., & Stegun, I. 1964, Handbook of Mathematical Functions (New York: Dover), 260
Akritas, M. G., & Bershady, M. A. 1996, ApJ, 470, 706
Caon, N., Capaccioli, M., & D'Onofrio, M. 1993, MNRAS, 265, 1013
Ferrarese, L., & Merritt, D. 2000, ApJ, 539, L9
Frei, Z., Guhathakurta, P., Gunn, J. E., & Tyson, J. A. 1996, AJ, 111, 174
Gebhardt, K., et al. 2000, ApJ, 539, L13
Graham, A. W. 1998, Ph.D. thesis, Australian National Univ., 72
Graham, A. W., Lauer, T. R., Colless, M. M., & Postman, M. 1996, ApJ, 465, 534
Graham, A. W., Trujillo, I., & Caon, N. 2001, AJ, 122, 1707
Hintzen, P., Angione, R., Talbert, F., Cheng, K.-P., Smith, E., & Stecher, T. P. 1993, in The Evolution of Galaxies and Their Environment, ed. D. Hollenbach, H. Thronson, & J. M. Shull (Moffett Field: NASA Ames), 38
Kent, S. M., Dame, T., & Fazio, G. 1991, ApJ, 378, 131
Kormendy, J., & Gebhardt, K. 2001, in AIP Conf. Proc. 586, 20th Texas Symp. on Relativistic Astrophysics, ed. H. Martel & J. C. Wheeler (New York: AIP), in press (astro-ph/0105230)
Kormendy, J., & Richstone, D. 1995, ARA&A, 33, 581
Maciejewski, W., & Binney, J. 2001, MNRAS, 323, 831
Magorrian, J., et al. 1998, AJ, 115, 2285
McLure, R. J., & Dunlop, J. S. 2001, MNRAS, submitted (astro-ph/0108417)
Merritt, D., & Ferrarese, L. 2001a, ApJ, 547, 140
———. 2001b, in ASP Conf. Ser. 249, The Central Kpc of Starbursts and AGN: The La Palma Connection, ed. J. H. Knapen, J. E. Beckman, I. Shlosman, & T. J. Mahoney (San Francisco: ASP), 335
Michard, R., & Marchal, J. 1994, A&AS, 105, 481
Press, W. H., Flannery, B. P., Teukolsky, S. A., & Vetterling, W. T. 1989, Numerical Recipes: The Art of Scientific Computing (New York: Cambridge Univ. Press)
Rest, A., et al. 2001, AJ, 121, 2431
Rix, H.-W., Carollo, C. M., & Freeman, K. 1999, ApJ, 513, L25
Sérsic, J.-L. 1968, Atlas de Galaxias Australes (Cordoba: Obs. Astron.)
Trujillo, I., Graham, A. W., & Caon, N. 2001, MNRAS, 326, 869
Wandel, A. 2002, ApJ, in press (astro-ph/0108461)